

# Coordinate descent heuristics for the irregular strip packing problem of rasterized shapes

Shunji Umetani\*, Shohei Murakami†

April 13, 2021

## Abstract

We consider the irregular strip packing problem of rasterized shapes, where a given set of pieces of irregular shapes represented in pixels should be placed into a rectangular container without overlap. The rasterized shapes enable us to check overlap without any exceptional handling due to geometric issues, while they often require much memory and computational effort in high-resolution. We develop an efficient algorithm to check overlap using a pair of scanlines that reduces the complexity of rasterized shapes by merging consecutive pixels in each row and column into strips with unit width, respectively. Based on this, we develop coordinate descent heuristics that repeat a line search in the horizontal and vertical directions alternately. Computational results for test instances show that the proposed algorithm obtains sufficiently dense layouts of rasterized shapes in high-resolution within a reasonable computation time.

**keyword:** packing, irregular strip packing problem, nesting problem, raster model, coordinate descent heuristics

## 1 Introduction

The *irregular strip packing problem* (ISP), or often called the *nesting problem*, is the one of the representative cutting and packing problems that emerges in a wide variety of industrial applications, such as garment manufacturing, sheet metal cutting, furniture making and shoe manufacturing [Alvarez-Valdes et al., 2018, Scheithauer, 2018]. This problem is categorized as the two-dimensional, irregular open dimensional problem in Dyckhoff [1990], Wäscher et al. [2007]. Given a set of pieces of irregular shapes and a rectangular container with a fixed width and a variable length, this problem asks a feasible layout of the pieces into the container such that no pair of pieces overlaps with each other and the container length is minimized. We note that rotations of pieces are usually restricted to a few number of degrees (e.g., 0 or 180 degrees) in many industrial applications, because textiles have grain and may have a drawing pattern. Figure 1 shows an instance of the ISP and a feasible solution.

The first issue encountered when handling the ISP is how to represent the irregular shapes. In computer graphics, the irregular shapes are often represented in two models as shown in Figure 2: the *vector model* represents an irregular shape as a set of chained line and curve segments forming its outline, and the *raster model* (also known as the *bitmap model*) represents an irregular shape as a set of grid pixels forming its inside. The vector model requires complex trigonometric computations with many exception handling for the intersection test of the irregular shapes,

---

\*Osaka University, Suita, Osaka, 565-0871, Japan. [umetani@ist.osaka-u.ac.jp](mailto:umetani@ist.osaka-u.ac.jp)

†Osaka University

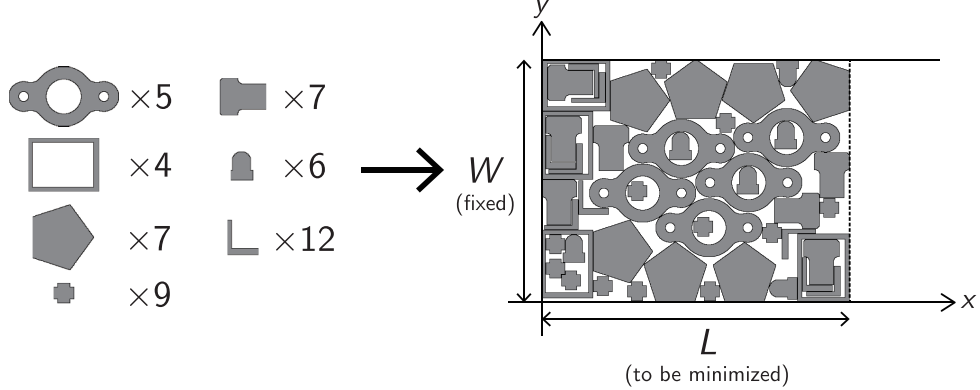


Figure 1: An instance of the irregular strip packing problem and its solution.

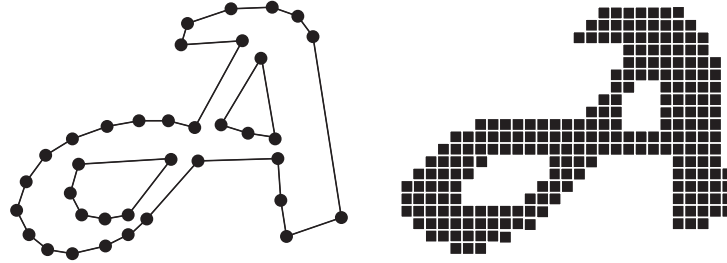


Figure 2: The vector and raster representations for an irregular shape.

while the raster model provides simple computations without any exception handling. On the other hand, the vector model often consumes less memory usage and computation time for the intersection test than the raster model, because the number of line and curve segments in the vector model often becomes much smaller than that of grid pixels in the raster model.

For the vector model, in particular polygons, the recent development of geometric techniques such as the no-fit polygon (NFP) enables us to compute their intersection test efficiently [Bennell and Oliveira, 2008, Leao et al., 2020]. Based on the efficient geometric computations, many efficient heuristic algorithms have been developed for the ISP of the polygons (called the polygon packing problem in this paper) [Bennell and Oliveira, 2009, Hu et al., 2018b]. A standard approach for the polygon packing problem is to develop construction algorithms, e.g., the bottom-left (BL) algorithm and the bottom-left fill (BLF) algorithm that places the pieces one by one into the container based on a given order [Albano and Sapuppo, 1980, Błazewicz et al., 1993, Oliveira et al., 2000, Dowsland et al., 2002, Gomes and Oliveira, 2002, Bennell and Song, 2010]. Another approach is to resort improvement algorithms that relocate pieces by solving the compaction problem and/or the separation problem [Li and Milenkovic, 1995, Bennell and Dowsland, 2001, Gomes and Oliveira, 2006]. The compaction problem relocates pieces from a given feasible placement so as to minimize the container length. The separation problem relocates pieces from a given infeasible placement so as to make it feasible while minimizing the total amount of their translation. The *overlap minimization problem* (OMP) is a variant of the separation problem that places pieces within the container with given width and length so as to minimize the overlap penalty for all pairs of pieces [Egeblad et al., 2007, Imamichi et al., 2009, Umetani et al., 2009, Leung et al., 2012, Elkeran, 2013].

Mundim et al. [2017] and Sato et al. [2019] constrained the search space to place the pieces on a discrete set of positions (i.e., a grid), and developed a discretized NFP called the no-fit raster for the intersection test of the irregular shapes. This constrained model of the search

space on a grid is called the dotted-board model [Toledo et al., 2013], which is similar to the raster model but different because the given pieces are represented in polygons (i.e., the vector model).

For the raster model, Oliveira and Ferreira [1993], Segenreich and Braga [1986] and Babu and Babu [2001] represented the pieces by matrices of different codes [Bennell and Oliveira, 2008]. The raster representations are simple to code the irregular shapes and provide simple procedures of counting the grid pixels for their intersection test, which enable us to develop practical software for a wide variety of free-form packing problems. However, their computational costs highly depend on the resolution of the raster representations; i.e., improving the resolution much increases the memory usage and computation time for the procedures. Based on these representations, several heuristic algorithms have been developed for the ISP of the raster model [Segenreich and Braga, 1986, Oliveira and Ferreira, 1993, Jain and Gea, 1998, Babu and Babu, 2001, Chen et al., 2004, Wong et al., 2009]. To improve the computational efficiency of the intersection test and the overlap minimization for the raster model, Okano [2002] and Hu et al. [2018a] proposed sophisticated data structures that merge the pixels of the irregular shapes into strips or rectangles. Despite these heuristic algorithms for the raster model, their numerical results were mainly for the instances of low-resolution and insufficient to convince their computational efficiency for the instances of high-resolution.

In this paper, we develop an efficient algorithm to compute the overlap penalty in the raster model. We propose a pair of scanlines representation for NFPs of the irregular shapes that reduces their complexity by merging consecutive pixels in each row and column into strips with unit width, respectively. Based on this, we develop coordinate descent heuristics (CDH) that repeat a line search in the horizontal and vertical directions alternately, where we introduced a corner detection technique used in computer vision [Rosten and Drummond, 2006] to reduce the search space of the line search. The coordinate descent heuristics are incorporated into a variant of the guided local search (GLS) for the OMP based on Umetani et al. [2009]. Using this as a main component, we then develop a heuristic algorithm for the ISP, which we call the *guided coordinate descent heuristics* (GCDH).

This paper is organized as follows. We first formulate the ISP and OMP in the raster model and illustrate the outline of the proposed algorithm GCDH for the ISP in Section 2. We then introduce an efficient intersection test for rasterized shapes in Section 3. We explain the main component of the proposed algorithm CDH for the OMP in Section 4 and the construction algorithm for an initial solution of the ISP in Section 5. Finally, we report computational results in Section 6 and make concluding remarks in Section 7.

## 2 Formulation and approach

### 2.1 Irregular strip packing problem of rasterized shapes

We are given a list of  $n$  pieces  $\mathcal{P} = \{P_1, P_2, \dots, P_n\}$  of rasterized shape with a list of their possible orientations  $\mathcal{O} = (O_1, O_2, \dots, O_n)$ , where a piece  $P_i$  can be rotated by  $o$  degrees for each  $o \in O_i$ . We assume without loss of generality that zero degree is always included in  $O_i$ . We are also given a rectangular container  $C = C(W, L)$  with a width  $W$  and a length  $L$ , where  $W$  is a non-negative constant and  $L$  is a non-negative variable. We assume that the container edges with the width  $W$  and the length  $L$  are parallel to the  $y$ -axis and the  $x$ -axis as shown in Figure 1, respectively, and the bottom-left corner of the container  $C$  is the origin  $(0, 0)$ . We denote a piece  $P_i$  rotated by  $o \in O_i$  degrees by  $P_i(o)$ , which may be written as  $P_i$  for simplicity when its orientation is not specified or clear from the context. We consider the bounding-box of a piece  $P_i(o_i)$  as the smallest rectangle that encloses  $P_i(o_i)$ , and its width and length are denoted by  $w_i(o_i)$  and  $l_i(o_i)$ ,

respectively. We describe a position of a piece  $P_i(o_i)$  by a coordinate  $\mathbf{v}_i = (x_i, y_i)$  of its reference point, where the reference point is the center of its bounding box. For convenience, we regard all pieces  $P_i$  as the set of grid pixels, when its reference point is put at the origin  $(0, 0)$ . We then describe a piece  $P_i$  placed at  $\mathbf{v}_i$  by the Minkowski sum

$$P_i \oplus \mathbf{v}_i = \{\mathbf{p} + \mathbf{v}_i \mid \mathbf{p} \in P_i\}. \quad (1)$$

We describe a solution of the ISP by lists of positions  $\mathbf{v} = (\mathbf{v}_1, \mathbf{v}_2, \dots, \mathbf{v}_n)$  and orientations  $\mathbf{o} = (o_1, o_2, \dots, o_n)$  of all pieces  $P_i$  ( $i = 1, \dots, n$ ). We note that a solution  $(\mathbf{v}, \mathbf{o})$  uniquely determines a layout of the pieces. The ISP is described as follows:

$$\begin{aligned} (\text{ISP}) \quad & \text{minimize} \quad L \\ & \text{subject to} \quad l_i(o_i)/2 \leq x_i \leq L - l_i(o_i)/2, \quad 1 \leq i \leq n, \\ & \quad w_i(o_i)/2 \leq y_i \leq W - w_i(o_i)/2, \quad 1 \leq i \leq n, \\ & \quad (P_i(o_i) \oplus \mathbf{v}_i) \cap (P_j(o_j) \oplus \mathbf{v}_j) = \emptyset, \quad 1 \leq i < j \leq n, \\ & \quad L \in \mathbb{R}_+, \\ & \quad \mathbf{v}_i = (x_i, y_i) \in \mathbb{R}_+^2, \quad 1 \leq i \leq n, \\ & \quad o_i \in O_i, \quad 1 \leq i \leq n, \end{aligned} \quad (2)$$

where  $\mathbb{R}_+$  is the set of nonnegative real values. We note that the coordinate  $\mathbf{v}_i = (x_i, y_i)$  of a piece  $P_i(o_i)$  takes  $(l_i(o_i)/2, w_i(o_i)/2)$  and  $(L - l_i(o_i)/2, W - w_i(o_i)/2)$  when it is placed at the bottom-left and top-right corners of the container  $C$ , respectively. We also note that minimization of the length  $L$  is equivalent to maximization of the density defined by  $\sum_{1 \leq i \leq n} (\text{area of } P_i) / WL$ .

## 2.2 Overlap minimization problem

We consider the OMP as a sub-problem of the ISP to find a feasible layout  $(\mathbf{v}, \mathbf{o})$  of given pieces for the container  $C$  with a given length  $L$ . A solution of the OMP may have a number of overlapping pieces, and the total amount of overlap is penalized in such a way that a solution with no penalty gives a feasible layout for the ISP. Let  $f_{ij}(\mathbf{v}_i, \mathbf{v}_j, o_i, o_j)$  be a function that measures the overlap amount for a pair of pieces  $P_i(o_i) \oplus \mathbf{v}_i$  and  $P_j(o_j) \oplus \mathbf{v}_j$ . The objective of the OMP is to find a solution  $(\mathbf{v}, \mathbf{o})$  that minimizes the total amount of the overlap penalty  $F(\mathbf{v}, \mathbf{o}) = \sum_{1 \leq i < j \leq n} f_{ij}(\mathbf{v}_i, \mathbf{v}_j, o_i, o_j)$  under the constraint that all pieces  $P_i$  ( $1 \leq i \leq n$ ) are placed within the container  $C(W, L)$ .

$$\begin{aligned} (\text{OMP}) \quad & \text{minimize} \quad F(\mathbf{v}, \mathbf{o}) = \sum_{1 \leq i < j \leq n} f_{ij}(\mathbf{v}_i, \mathbf{v}_j, o_i, o_j) \\ & \text{subject to} \quad l_i(o_i)/2 \leq x_i \leq L - l_i(o_i)/2, \quad 1 \leq i \leq n, \\ & \quad w_i(o_i)/2 \leq y_i \leq W - w_i(o_i)/2, \quad 1 \leq i \leq n, \\ & \quad \mathbf{v}_i = (x_i, y_i) \in \mathbb{R}_+^2, \quad 1 \leq i \leq n, \\ & \quad o_i \in O_i, \quad 1 \leq i \leq n. \end{aligned} \quad (3)$$

We introduce the *directional penetration depth* to define the overlap penalty function  $f_{ij}(\mathbf{v}_i, \mathbf{v}_j, o_i, o_j)$  for a pair of pieces  $P_i(o_i) \oplus \mathbf{v}_i$  and  $P_j(o_j) \oplus \mathbf{v}_j$ . The directional penetration depth  $\delta(P_i, P_j, \mathbf{d})$  is defined as the minimum translational distance in a given direction  $\mathbf{d}$  ( $\|\mathbf{d}\| = 1, \mathbf{d} \in \mathbb{R}^2$ ) to separate a pair of pieces  $P_i$  and  $P_j$  [Dobkin et al., 1993]. If they do not overlap, then their directional penetration depth is zero. The formal definition of the directional penetration depth is given by

$$\delta(P_i, P_j, \mathbf{d}) = \min\{|t| \mid P_i \cap (P_j \oplus t\mathbf{d}) = \emptyset, t \in \mathbb{R}\}. \quad (4)$$

In this paper, we define the overlap penalty  $f_{ij}(\mathbf{v}_i, \mathbf{v}_j, o_i, o_j)$  for a pair of pieces  $P_i(o_i) \oplus \mathbf{v}_i$  and  $P_j(o_j) \oplus \mathbf{v}_j$  as the minimum within the horizontal and vertical penetration depths

$$f_{ij}(\mathbf{v}_i, \mathbf{v}_j, o_i, o_j) = \min\{\delta(P_i(o_i) \oplus \mathbf{v}_i, P_j(o_j) \oplus \mathbf{v}_j, \mathbf{d}) \mid \mathbf{d} \in \{(1, 0), (0, 1)\}\}. \quad (5)$$

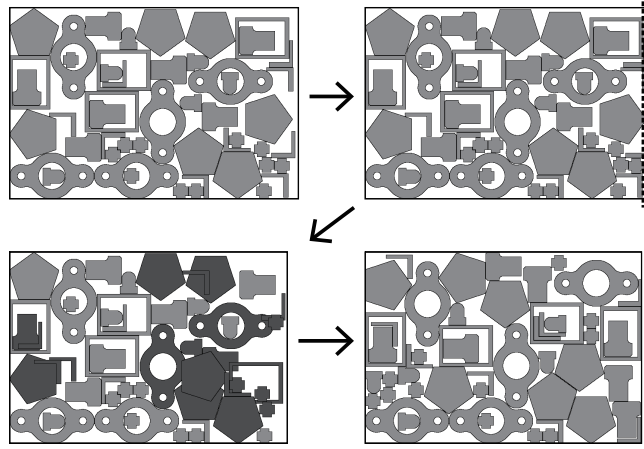


Figure 3: The outline of the proposed algorithm.

### 2.3 Entire algorithm algorithm for the irregular strip packing problem

We give an entire description of the proposed algorithm GCDH for the ISP. The GCDH first generates an initial solution  $(\mathbf{v}, \mathbf{o})$  by a construction algorithm to be explained in Section 5, and sets the minimum container length  $L$  containing all pieces  $P_i$  ( $1 \leq i \leq n$ ). It then searches the minimum feasible container length  $L^*$  by shrinking or extending the right sides of the container  $C$  until the time limit is reached, where the ratios of shrinking and extending container length are controlled by the parameters  $r_{\text{dec}}$  and  $r_{\text{inc}}$ , respectively. If the current solution  $(\mathbf{v}, \mathbf{o})$  is feasible, then it shrinks the container length  $L$  to  $(1 - r_{\text{dec}})L$  and relocates protruding pieces  $P_i$  at random positions in the container  $C(W, L)$ ; otherwise it extends the container length  $L$  to  $(1 + r_{\text{inc}})L$ . If there is at least one overlapping pair of pieces in the current solution, then it tries to resolve overlap by the CDH for the OMP explained in Section 4. Figure 3 shows the outline of the proposed algorithm GCDH. The algorithm is formally described in Algorithm 1, where we omit the input data  $W, \mathcal{P}, \mathcal{O}$  commonly used in all algorithms in this paper.

---

#### Algorithm 1 GCDH

---

```

1:  $L, (\mathbf{v}, \mathbf{o}) \leftarrow \text{CONSTRUCT}$  {See Algorithm 5}
2:  $L^* \leftarrow L, (\mathbf{v}^*, \mathbf{o}^*) \leftarrow (\mathbf{v}, \mathbf{o})$ 
3:  $L \leftarrow (1 - r_{\text{dec}})L^*$ 
4: repeat
5:    $(\mathbf{v}, \mathbf{o}) \leftarrow \text{GLS}(L, \mathbf{v}, \mathbf{o})$  {See Algorithm 4}
6:   if  $(\mathbf{v}, \mathbf{o})$  is feasible then
7:      $L^* \leftarrow L, (\mathbf{v}^*, \mathbf{o}^*) \leftarrow (\mathbf{v}, \mathbf{o})$ 
8:      $L \leftarrow (1 - r_{\text{dec}})L^*$ 
9:     Relocate protruding pieces  $P_i(o_i)$  at random position in  $C(W, L)$ .
10:  else
11:     $L \leftarrow (1 + r_{\text{inc}})L$ 
12:    if  $L \geq L^*$  then
13:       $L \leftarrow (1 - r_{\text{dec}})L^*, (\mathbf{v}, \mathbf{o}) \leftarrow (\mathbf{v}^*, \mathbf{o}^*)$ 
14:      Relocate protruding pieces  $P_i(o_i)$  at random position in  $C(W, L)$ .
15:  until The time limit is reached
16:  Return  $(\mathbf{v}^*, \mathbf{o}^*)$ 

```

---

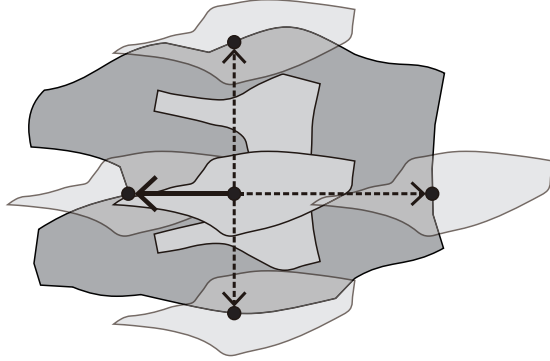


Figure 4: The no-fit polygon  $\text{NFP}(P_i, P_j)$  for two irregular shapes  $P_i$  and  $P_j$ .



Figure 5: The horizontal and vertical scanline representations for a rasterized shape.

### 3 Intersection test for rasterized shapes via scanline representation

#### 3.1 No-fit polygon for intersection test

The *no-fit polygon* (NFP) introduced by Art [1966] is a representative geometric technique used in many algorithms for the polygon packing problem. It is also used for other applications such as image processing and robot motion planning, and is also known as the Minkowski difference and the configuration-space obstacle, respectively. The no-fit polygon  $\text{NFP}(P_i, P_j)$  of an ordered pair of pieces  $P_i$  and  $P_j$  is defined by

$$\text{NFP}(P_i, P_j) = P_i \oplus (-P_j) = \{\mathbf{u} - \mathbf{w} \mid \mathbf{u} \in P_i, \mathbf{w} \in P_j\}. \quad (6)$$

The NFP has an important property that  $P_j \oplus \mathbf{v}_j$  overlaps with  $P_i \oplus \mathbf{v}_i$  if and only if  $\mathbf{v}_j - \mathbf{v}_i \in \text{NFP}(P_i, P_j)$  holds. That is, the intersection test for two irregular shapes  $P_i \oplus \mathbf{v}_i$  and  $P_j \oplus \mathbf{v}_j$  can be identified by testing whether a point  $\mathbf{v}_j - \mathbf{v}_i$  is inside an irregular shape  $\text{NFP}(P_i, P_j)$  or not. Figure 4 shows an example of  $\text{NFP}(P_i, P_j)$  for two irregular shapes  $P_i$  and  $P_j$ . The NFP enables us to compute the intersection test and the directed penetration depth efficiently, assuming that we compute NFPs for all pairs of pieces in advance.

#### 3.2 Scanline representation for rasterized shapes

We consider the horizontal and vertical scanline representations that reduce the complexity of rasterized shapes by merging consecutive pixels in each row and column into strips with unit width, respectively. Figure 5 shows an example of the horizontal and vertical scanline representations of a rasterized shape. Hu et al. [2018a] developed an efficient algorithm to compute the scanline representation of  $\text{NFP}(P_i, P_j)$ . Based on these, we compute the horizontal penetration depth  $\delta(P_i \oplus \mathbf{v}_i, P_j \oplus \mathbf{v}_j, (1, 0))$  efficiently. Let  $\mathcal{S}_{ij} = \{S_{ij1}, S_{ij2}, \dots, S_{ijm_{ij}}\}$  be the

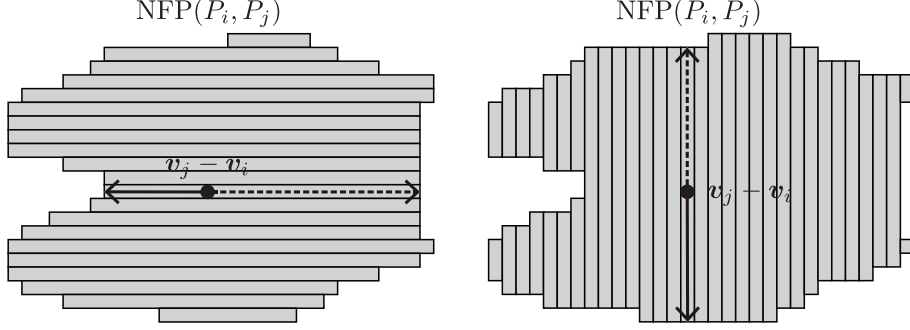


Figure 6: Computing the horizontal and vertical penetration depths from the scanline representations of NFP.

set of horizontal strips representing  $\text{NFP}(P_i, P_j)$ , where  $m_{ij}$  is the number of strips representing an  $\text{NFP}(P_i, P_j)$ . When the relative position  $\mathbf{v}_j - \mathbf{v}_i$  of the piece  $P_j$  is placed in a strip  $S_{ijk}$ , the horizontal penetration depth  $\delta(P_i \oplus \mathbf{v}_i, P_j \oplus \mathbf{v}_j, (1, 0))$  then takes the minimum length from  $\mathbf{v}_j - \mathbf{v}_i$  to left and right side of the strip  $S_{ijk}$ . We note that the horizontal penetration depth can be computed in  $O(1)$  time when  $\text{NFP}(P_i, P_j)$  is  $y$ -monotone, where a rasterized shape is  $y$ -monotone if it can be represented by a set of strips such that there is exactly one strip for each row and strips in adjacent rows are contiguous. We also compute the vertical penetration depth  $\delta(P_i \oplus \mathbf{v}_i, P_j \oplus \mathbf{v}_j, (0, 1))$  efficiently utilizing the vertical scanline representation of  $\text{NFP}(P_i, P_j)$  in the same fashion. Figure 6 shows an example of computing the horizontal and vertical penetration depths from the scanline representations of NFP.

## 4 Coordinate descent heuristics for the overlap minimization problem

### 4.1 Outline of the coordinate descent heuristics

We develop an iterative algorithm for the OMP called the *coordinate descent heuristics* (CDH), which start from an initial solution and repeatedly apply the *line search* that minimizes the objective function along a coordinate direction until no better solution is found in any coordinate direction.

We first explain the neighborhood of the CDH for the OMP. Let  $(\mathbf{v}, \mathbf{o})$  be the current solution. The neighborhood  $\text{NB}(\mathbf{v}, \mathbf{o})$  is defined as the set of neighbor solutions, where a neighbor solution  $(\mathbf{v}', \mathbf{o}') \in \text{NB}(\mathbf{v}, \mathbf{o})$  is obtained by setting a new orientation  $o'_k \in O_k$  of a piece  $P_k$  ( $1 \leq k \leq n$ ) and iteratively applying the line search to find a new position  $\mathbf{v}'_k$ . The quality of a solution  $(\mathbf{v}, \mathbf{o})$  is measured by the following weighted overlap penalty function

$$\tilde{F}(\mathbf{v}, \mathbf{o}) = \sum_{1 \leq i < j \leq n} \alpha_{ij} \cdot f_{ij}(\mathbf{v}_i, \mathbf{v}_j, o_i, o_j), \quad (7)$$

where  $\alpha_{ij} > 0$  are the penalty weights and  $f_{ij}$  are the overlap penalties defined in (5) for a pair of pieces  $P_i(o_i) \oplus \mathbf{v}_i$  and  $P_j(o_j) \oplus \mathbf{v}_j$ . The penalty weights  $\alpha_{ij}$  are adaptively controlled by the GLS to be explained in Section 4.3. For a piece  $P_k(o'_k)$ , the neighborhood search finds a new position  $\mathbf{v}'_k$  in the container  $C(W, L)$  such that the following weighted overlap penalty function

$$\tilde{F}_k(\mathbf{v}'_k, o'_k) = \sum_{1 \leq j \leq n, j \neq k} \alpha_{kj} \cdot f_{kj}(\mathbf{v}'_k, \mathbf{v}_j, o'_k, o_j) \quad (8)$$

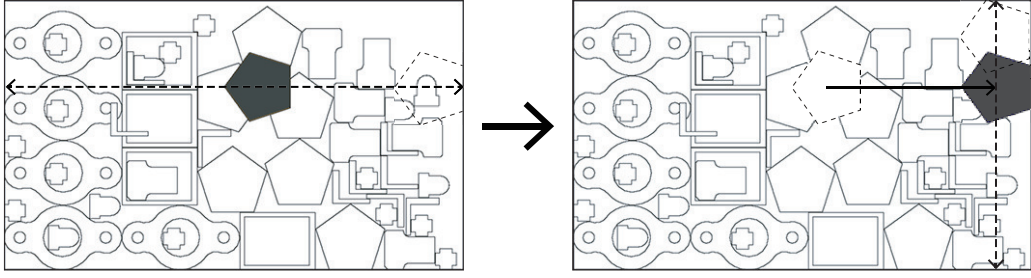


Figure 7: The neighborhood search of the CDH for the OMP.

is minimized. For this, the neighborhood search repeatedly moves the piece  $P_k(o'_k)$  in the horizontal and vertical directions alternately until no better position is found in either direction. Figure 7 shows how the neighborhood search proceeds. For each move of the piece  $P_k(o'_k)$  in a specified direction  $\mathbf{d} \in \{(1, 0), (0, 1)\}$ , let

$$N = \{t \mid P(o'_k) \oplus (\mathbf{v}_k + t\mathbf{d}) \subseteq C(W, L), t \in \mathbb{Z}\} \quad (9)$$

be the set of valid  $t$  such that the piece  $P_k(o'_k)$  placed on the line  $\mathbf{v}_k + t\mathbf{d}$  ( $t \in \mathbb{Z}$ ) is contained in the container  $C(W, L)$ , where  $\mathbb{Z}$  is the set of integer values. The line search (to be explained in Section 4.2) finds a new valid position  $\mathbf{v}'_k = \mathbf{v}_k + t\mathbf{d}$  ( $t \in N$ ) that minimizes the overlap penalty function  $\tilde{F}_k(\mathbf{v}_k + t\mathbf{d}, o'_k)$ . The neighborhood search is formally described in Algorithm 2.

---

**Algorithm 2** NEIGHBORSEARCH( $L, \mathbf{v}, \mathbf{o}, P_k, o'_k$ )

---

```

1:  $\mathbf{v}' \leftarrow \mathbf{v}$ ,  $o'_j \leftarrow o_j$  ( $j \neq k$ ),  $\mathbf{d} \leftarrow (1, 0)$ 
2: Find  $t \in N$  to minimize  $\tilde{F}_k(\mathbf{v}'_k + t\mathbf{d}, o'_k)$ 
3: if  $\tilde{F}_k(\mathbf{v}'_k + t\mathbf{d}, o'_k) < \tilde{F}_k(\mathbf{v}'_k, o'_k)$  then
4:    $\mathbf{v}'_k \leftarrow \mathbf{v}'_k + t\mathbf{d}$ 
5:  $\mathbf{d} \leftarrow (0, 1)$ 
6: repeat
7:   Find  $t \in N$  to minimize  $\tilde{F}_k(\mathbf{v}'_k + t\mathbf{d}, o'_k)$ 
8:   if  $\tilde{F}_k(\mathbf{v}'_k + t\mathbf{d}, o'_k) < \tilde{F}_k(\mathbf{v}'_k, o'_k)$  then
9:      $\mathbf{v}'_k \leftarrow \mathbf{v}'_k + t\mathbf{d}$ 
10:    if  $\mathbf{d} = (1, 0)$  then
11:       $\mathbf{d} \leftarrow (0, 1)$ 
12:    else
13:       $\mathbf{d} \leftarrow (1, 0)$ 
14: until  $\tilde{F}_k(\mathbf{v}'_k + t\mathbf{d}, o'_k) = \tilde{F}_k(\mathbf{v}'_k, o'_k)$ 
15: Return  $(\mathbf{v}', \mathbf{o}')$ 

```

---

We now describe the outline of the CDH for the OMP. Starting from an initial solution  $(\mathbf{v}, \mathbf{o})$  with some overlapping pieces, the CDH repeatedly replaces the current solution  $(\mathbf{v}, \mathbf{o})$  with the first improved solution  $(\mathbf{v}', \mathbf{o}') \in \text{NB}(\mathbf{v}, \mathbf{o})$  obtained by the neighborhood search. That is, the CDH searches  $\text{NB}(\mathbf{v}, \mathbf{o})$  in random order, and if it finds an improved solution  $(\mathbf{v}', \mathbf{o}') \in \text{NB}(\mathbf{v}, \mathbf{o})$  satisfying  $\tilde{F}(\mathbf{v}', \mathbf{o}') < \tilde{F}(\mathbf{v}, \mathbf{o})$ , then it immediately replaces the current solution  $(\mathbf{v}, \mathbf{o})$  with  $(\mathbf{v}', \mathbf{o}')$ . If no overlapping piece exists in the current solution  $(\mathbf{v}, \mathbf{o})$  (i.e.,  $\tilde{F}(\mathbf{v}, \mathbf{o}) = 0$ ) or no better solution found in  $\text{NB}(\mathbf{v}, \mathbf{o})$ , then the CDH outputs  $(\mathbf{v}, \mathbf{o})$  as a locally optimal solution and the best solution  $(\mathbf{v}^*, \mathbf{o}^*)$  obtained so far, measured by the original penalty function  $F$ , and halts.

We also incorporate the *fast local search* (FLS) strategy [Voudouris and Tsang, 1999] to improve the efficiency of the CDH. The strategy decomposes the neighborhood into a number

of subneighborhoods, which are labeled active or inactive depending on whether they are being searched or not, i.e., it skips evaluating all neighbor solutions in inactive subneighborhoods. We define the subneighborhood  $\text{NB}_k(\mathbf{v}, \mathbf{o})$  ( $1 \leq k \leq n$ ) of the current solution  $(\mathbf{v}, \mathbf{o})$  as the set of solutions obtainable by setting orientation  $o'_k \in O_k$  and applying the neighborhood search to the piece  $P_k$ , i.e., the neighborhood  $\text{NB}(\mathbf{v}, \mathbf{o})$  is partitioned with respect to the pieces  $P_k$  ( $1 \leq k \leq n$ ). The CDH first sets all subneighborhoods  $\text{NB}_k(\mathbf{v}, \mathbf{o})$  ( $1 \leq k \leq n$ ) to be active, and it searches active subneighborhoods  $\text{NB}_k(\mathbf{v}, \mathbf{o})$  in random order. If no improvement has been made in an active subneighborhood  $\text{NB}_k(\mathbf{v}, \mathbf{o})$ , then the CDH inactivates it. If the CDH finds an improved solution  $(\mathbf{v}', \mathbf{o}')$  satisfying  $\tilde{F}(\mathbf{v}', \mathbf{o}') < \tilde{F}(\mathbf{v}, \mathbf{o})$  in an active subneighborhood  $\text{NB}_k(\mathbf{v}, \mathbf{o})$ , then it activates all subneighborhood  $\text{NB}_j(\mathbf{v}, \mathbf{o})$  corresponding to the pieces  $P_j$  overlapping with the piece  $P_k$  before and after its move. The CDH is formally described in Algorithm 3, where  $A$  denotes the set of indices  $k$  ( $1 \leq k \leq n$ ) corresponding to the active subneighborhood  $\text{NB}_k(\mathbf{v}, \mathbf{o})$ , and  $(\mathbf{v}^*, \mathbf{o}^*)$  and  $(\tilde{\mathbf{v}}, \tilde{\mathbf{o}})$  denote the best solutions of the original overlap penalty function  $F$  and the weighted overlap penalty function  $\tilde{F}$ , respectively.

---

**Algorithm 3**  $\text{CDH}(L, \mathbf{v}, \mathbf{o})$ 


---

```

1:  $(\tilde{\mathbf{v}}, \tilde{\mathbf{o}}) \leftarrow (\mathbf{v}, \mathbf{o})$ ,  $(\mathbf{v}^*, \mathbf{o}^*) \leftarrow (\mathbf{v}, \mathbf{o})$ ,  $A \leftarrow \{1, \dots, n\}$ 
2: while  $A \neq \emptyset$  do
3:   Randomly select  $k \in A$ 
4:    $O \leftarrow O_k$ 
5:   while  $O \neq \emptyset$  do
6:     Randomly select  $o'_k \in O$ 
7:      $(\mathbf{v}', \mathbf{o}') \leftarrow \text{NEIGHBORSEARCH}(L, \mathbf{v}, \mathbf{o}, P_k, o'_k)$  {See Algorithm 2}
8:     if  $F(\mathbf{v}', \mathbf{o}') < F(\mathbf{v}^*, \mathbf{o}^*)$  then
9:        $(\mathbf{v}^*, \mathbf{o}^*) \leftarrow (\mathbf{v}', \mathbf{o}')$ 
10:      if  $F(\mathbf{v}^*, \mathbf{o}^*) = 0$  then
11:        Return  $(\mathbf{v}^*, \mathbf{o}^*)$ ,  $(\tilde{\mathbf{v}}, \tilde{\mathbf{o}})$ 
12:      if  $\tilde{F}(\mathbf{v}', \mathbf{o}') < \tilde{F}(\tilde{\mathbf{v}}, \tilde{\mathbf{o}})$  then
13:         $(\tilde{\mathbf{v}}, \tilde{\mathbf{o}}) \leftarrow (\mathbf{v}', \mathbf{o}')$ 
14:        for  $P_j$  overlapping with  $P_k$  before and after the move do
15:           $A \leftarrow A \cup \{j\}$ 
16:           $O \leftarrow O \setminus \{o'_k\}$ 
17:         $A \leftarrow A \setminus \{k\}$ 
18:  Return  $(\mathbf{v}^*, \mathbf{o}^*)$ ,  $(\tilde{\mathbf{v}}, \tilde{\mathbf{o}})$ 

```

---

## 4.2 Efficient implementation of the line search

We develop an efficient line search algorithm for the neighborhood search, which finds a new position when a piece  $P_k(o'_k)$  moves in a specified direction  $\mathbf{d} \in \{(1, 0), (0, 1)\}$ . Recall that the line search finds the new position  $\mathbf{v}'_k = \mathbf{v}_k + t\mathbf{d}$  to minimize the overlap penalty function  $\tilde{F}_k(\mathbf{v}_k + t\mathbf{d}, o'_k)$  while the piece  $P_k(o'_k)$  is contained in the container  $C(W, L)$ . We consider below the case when  $P_k(o'_k)$  moves in the horizontal direction (i.e.,  $\mathbf{d} = (1, 0)$ ). The case of the vertical direction (i.e.,  $\mathbf{d} = (0, 1)$ ) is almost the same and is omitted. The overlap penalty function  $\tilde{F}_k(\mathbf{v}_k + t\mathbf{d}, o'_k)$  is decomposed into  $f_{kj}(\mathbf{v}_k + t\mathbf{d}, \mathbf{v}_j, o'_k, o_j)$  for pairs of pieces  $P_k(o'_k)$  and  $P_j(o_j)$  ( $1 \leq j \leq n, j \neq k$ ) by definition (8). Let

$$I_{kj} = \{t \mid \mathbf{v}_k + t\mathbf{d} \in \text{NFP}(P_j(o_j), P_k(o'_k)), t \in N\} \quad (10)$$

be the set of positions of the piece  $P_k(o'_k)$  in terms of  $t \in N$  such that it overlaps with the other piece  $P_j(o_j)$ . If  $I_{kj} = \emptyset$  holds, then the overlap penalty  $f_{kj}(\mathbf{v}_k + t\mathbf{d}, \mathbf{v}_j, o'_k, o_j)$  always takes zero

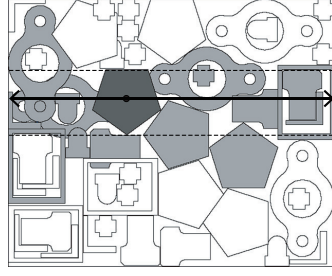


Figure 8: Detecting the overlapping pieces in the line search.

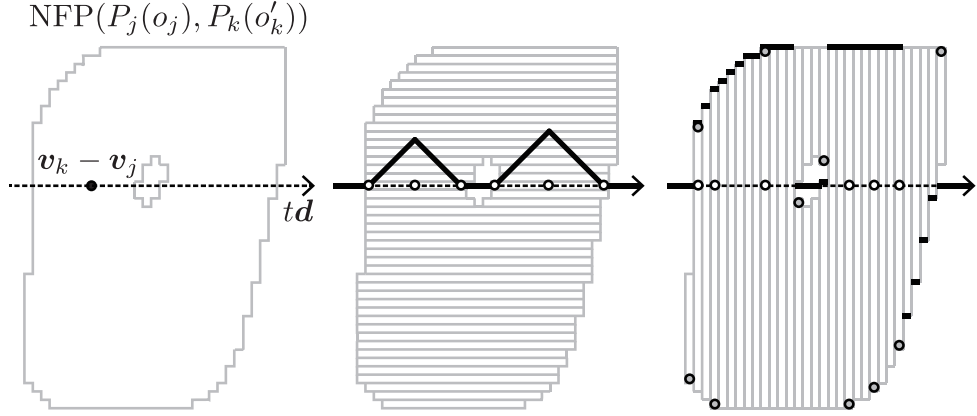


Figure 9: Computing the horizontal and vertical penetration depth in the line search.

for  $t \in N$ . The line search algorithm first detects whether  $I_{kj} = \emptyset$  or not by checking the overlap between projections of pieces  $P_k(o'_k) \oplus \mathbf{v}_k$  and  $P_j(o_j) \oplus \mathbf{v}_j$  onto the  $y$ -axis. That is,  $I_{kj} = \emptyset$  holds if and only if the intersection of their projections satisfies  $(y_k^{\min}, y_k^{\max}) \cap (y_j^{\min}, y_j^{\max}) = \emptyset$ , where  $y_i^{\min}$  and  $y_i^{\max}$  ( $1 \leq i \leq n$ ) of a piece  $P_i(o_i) \oplus \mathbf{v}_i$  are defined by

$$y_i^{\min} = \min\{y \mid (x, y) \in P_i(o_i) \oplus \mathbf{v}_i\}, \quad (11)$$

$$y_i^{\max} = \max\{y \mid (x, y) \in P_i(o_i) \oplus \mathbf{v}_i\}, \quad (12)$$

respectively. Figure 8 shows an example of detecting the overlapping pieces  $P_j(o_j)$  when the piece  $P_k(o'_k)$  moves in the horizontal direction. Let  $N^+ = \bigcup_{1 \leq j \leq n, j \neq k} I_{kj}$  be the set of  $t \in N$  inducing overlap with other pieces, and  $N^- = N \setminus N^+$  be its complement. If  $N^- \neq \emptyset$  holds, then the line search algorithm finds the minimum  $t \in N^-$  (i.e., the left most feasible position); otherwise, it finds the position  $t \in N^+$  that minimizes the overlap penalty function  $\tilde{F}_k(\mathbf{v}_k + t\mathbf{d}, o'_k)$ .

We now consider how to compute the overlap penalty function  $f_{kj}(\mathbf{v}_k + t\mathbf{d}, \mathbf{v}_j, o'_k, o_j)$  defined in (5) for a given  $t \in N$ , where  $I_{kj} \neq \emptyset$  is assumed. Let  $\mathbf{v}'_k = \mathbf{v}_k + t\mathbf{d}$  be the position of the piece  $P_k(o'_k)$  for a given  $t \in N$ . If  $t \notin I_{kj}$  holds, then  $f_{kj}(\mathbf{v}'_k, \mathbf{v}_j, o'_k, o_j) = 0$ ; otherwise, the overlap penalty  $f_{kj}(\mathbf{v}'_k, \mathbf{v}_j, o'_k, o_j)$  is decomposed into the horizontal and vertical penetration depths as shown in Figure 9. We denote the horizontal and vertical penetration depths for a given  $t \in N$  by

$$\delta(P_k(o'_k) \oplus \mathbf{v}'_k, P_j(o_j) \oplus \mathbf{v}_j, \mathbf{d}) = \min\{|s| \mid \mathbf{v}'_k - \mathbf{v}_j + s\mathbf{d} \notin \text{NFP}(P_j(o_j), P_k(o'_k))\}, \quad (13)$$

for  $\mathbf{d} \in \{(1, 0), (0, 1)\}$ , respectively. Recall the horizontal and vertical scanline representations of  $\text{NFP}(P_j(o_j), P_k(o'_k))$  in Figure 6. When the relative position  $\mathbf{v}'_k - \mathbf{v}_j$  of the piece  $P_k(o'_k)$  is placed

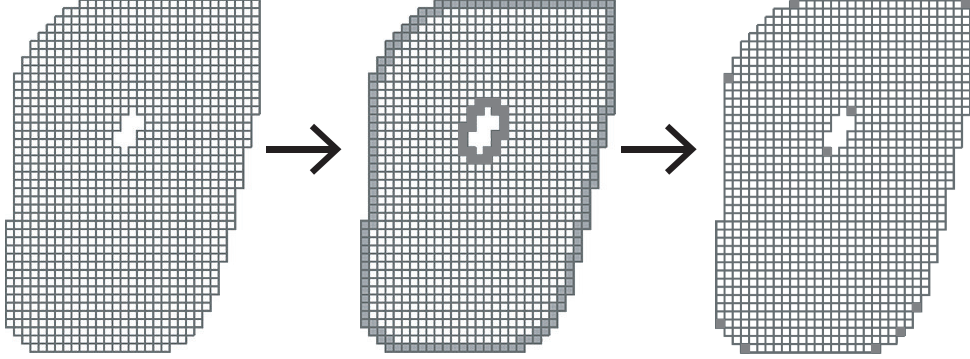


Figure 10: The corner detection algorithm for the NFP.

in a strip, the horizontal (resp., vertical) penetration depth then takes the minimum horizontal distance  $|s|$  from  $\mathbf{v}'_k - \mathbf{v}_j$  to left and right (resp., bottom and top) side of the strip.

The line search algorithm computes the overlap penalty  $\tilde{F}_k(\mathbf{v}_k + t\mathbf{d}, o'_k)$  for all  $t \in N^+$  when  $N^- = \emptyset$  holds. It is very time consuming when  $|N^+|$  becomes larger according to high-resolution of the raster representation. The horizontal penetration depth is a simple piecewise linear function that can be easily computed, while the vertical penetration depth is a complicated stepwise function that often changes rapidly as shown in Figure 9. However, the rapid changes of the vertical penetration depth only occur at the corners of  $\text{NFP}(P_j(o_j), P_k(o'_k))$ . We accordingly focus a corner detection technique to reduce the search space  $N$  of the line search algorithm. We first detect the contour of  $\text{NFP}(P_j(o_j), P_k(o'_k))$  and then apply a fast corner detection algorithm called FAST [Rosten and Drummond, 2006] to the contour as shown in Figure 10. Let  $\overline{\text{NFP}}(P_j(o_j), P_k(o'_k))$  be the set of detected corners in  $\text{NFP}(P_j(o_j), P_k(o'_k))$  obtained by the FAST. We now consider the projection  $\bar{I}_{kj}$  of  $\overline{\text{NFP}}(P_j(o_j), P_k(o'_k))$  onto the horizontal line  $\mathbf{v}_k + t\mathbf{d}$  ( $t \in N$ ) and  $\bar{N}^+ = \bigcup_{1 \leq j \leq n, j \neq k} \bar{I}_{kj}$ . The line search algorithm computes the overlap penalty  $\tilde{F}_k(\mathbf{v}_k + t\mathbf{d}, o'_k)$  only for  $t \in \bar{N}^+$  (instead of  $N^+$ ) when  $N^- = \emptyset$  holds. The white nodes in Figure 9 represent the positions  $\mathbf{v}_k + t\mathbf{d} - \mathbf{v}_j$  ( $t \in \bar{I}_{kj}$ ) of the piece  $P_k(o'_k)$  to be evaluated by the line search algorithm.

### 4.3 Guided local search

It is often the case that the CDH alone may not attain a sufficiently good solution. To improve its performance, we incorporate it into one of the representative metaheuristics called the *guided local search* (GLS) [Voudouris and Tsang, 1999]. The GLS repeats the CDH while updating the penalty weights of the objective function adaptively to resume the search from the previous locally optimal solution. The GLS starts from an initial solution  $(\mathbf{v}, \mathbf{o})$  with some overlapping pieces, where the penalty weights  $\alpha_{ij}$  are initialized to 1.0. Whenever the CDH stops at a locally optimal solution  $(\mathbf{v}, \mathbf{o})$ , the GLS updates the penalty weights  $\alpha_{ij}$  by the following formula:

$$\alpha_{ij} \leftarrow \alpha_{ij} + \frac{f_{ij}(\mathbf{v}_i, \mathbf{v}_j, o_i, o_j)}{\max_{1 \leq k < l \leq n} f_{kl}(\mathbf{v}_k, \mathbf{v}_l, o_k, o_l)}, \quad 1 \leq i < j \leq n. \quad (14)$$

By updating the penalty weights  $\alpha_{ij}$  ( $1 \leq i < j \leq n$ ) repeatedly, the current solution  $(\mathbf{v}, \mathbf{o})$  becomes no longer locally optimal under the updated overlap penalty function  $\tilde{F}$ , and the GLS resumes the search from the current solution. The GLS stops these operations if it fails to improve the best solution  $(\mathbf{v}^*, \mathbf{o}^*)$  of the original penalty function  $F$  after a specified number  $k_{\max}$  of consecutive calls to the CDH. The GLS is formally described in Algorithm 4.

---

**Algorithm 4** GLS( $L, \mathbf{v}, \mathbf{o}$ )

---

```
1:  $(\tilde{\mathbf{v}}, \tilde{\mathbf{o}}) \leftarrow (\mathbf{v}, \mathbf{o})$ ,  $(\mathbf{v}^*, \mathbf{o}^*) \leftarrow (\mathbf{v}, \mathbf{o})$ ,  $\alpha_{ij} \leftarrow 1.0$  ( $1 \leq i < j \leq n$ ),  $k \leftarrow 0$ 
2: while  $k < k_{\max}$  do
3:    $(\mathbf{v}', \mathbf{o}')$ ,  $(\tilde{\mathbf{v}}, \tilde{\mathbf{o}}) \leftarrow \text{CDH}(L, \tilde{\mathbf{v}}, \tilde{\mathbf{o}})$  {See Algorithm 3}
4:   if  $F(\mathbf{v}', \mathbf{o}') < F(\mathbf{v}^*, \mathbf{o}^*)$  then
5:      $(\mathbf{v}^*, \mathbf{o}^*) \leftarrow (\mathbf{v}', \mathbf{o}')$ ,  $k \leftarrow 0$ 
6:     if  $F(\mathbf{v}^*, \mathbf{o}^*) = 0$  then
7:       Return  $(\mathbf{v}^*, \mathbf{o}^*)$ 
8:     Update the penalty weights  $\alpha_{ij}$  ( $1 \leq i < j \leq n$ ) of  $(\tilde{\mathbf{v}}, \tilde{\mathbf{o}})$  by (14)
9:    $k \leftarrow k + 1$ 
10:  Return  $(\mathbf{v}^*, \mathbf{o}^*)$ 
```

---

## 5 Construction algorithm for the initial layout

We generate an initial solution  $(\mathbf{v}, \mathbf{o})$  for the ISP using the next-fit decreasing height (NFDH) algorithm. The NFDH is a variant of the level algorithms for the rectangle packing problem [Hu et al., 2018b] that places rectangle pieces from bottom to top in columns forming levels as shown in Figure 11. The first level is the left side of the container, and each subsequent level is along the vertical line coinciding with the right of the longest piece placed in the previous level. The NFDH first sorts the pieces  $P_i$  ( $1 \leq i \leq n$ ) in the descending order of the lengths  $l_i$  of their bounding-boxes, where they are not rotated (i.e.,  $l_i = l_i(0)$ ). Let the container length  $L$  be sufficiently long, e.g.,  $L > \sum_{1 \leq i \leq n} l_i$ . The NFDH places all pieces  $P_i$  ( $1 \leq i \leq n$ ) one by one into the container  $C$  according to the above order. If possible, each piece  $P_i$  (more precisely, its bounding-box) is placed at the bottom-most feasible position in the current level; otherwise, a new level is created to place the piece  $P_i$ . We then apply a compaction algorithm (called COMPACT) based on the bottom-left strategy that makes successive sliding moves to the left and the bottom alternately as long as possible. The compaction algorithm can be implemented based on the neighborhood search (Algorithm 2) by replacing the condition  $\tilde{F}_k(\mathbf{v}'_k + t\mathbf{d}, \mathbf{o}'_k) < \tilde{F}_k(\mathbf{v}'_k, \mathbf{o}'_k)$  with  $t < 0$  (i.e., the piece  $P_k$  slides to the left or the bottom without overlap).

---

**Algorithm 5** CONSTRUCT

---

```
1:  $L \leftarrow 0$ ,  $\bar{L} \leftarrow 0$ ,  $\bar{w} \leftarrow 0$ 
2: for  $P_i$  ( $1 \leq i \leq n$ ) in the descending order of  $l_i$  do
3:   if  $\bar{w} + w_i > W$  then
4:      $L \leftarrow L + \bar{L}$ ,  $\bar{w} \leftarrow 0$ ,  $\bar{L} \leftarrow 0$ 
5:    $\mathbf{v}_i \leftarrow (L + \frac{l_i}{2}, \bar{w} + \frac{w_i}{2})$ ,  $\bar{w} \leftarrow \bar{w} + w_i$ ,  $\bar{L} \leftarrow \max\{\bar{L}, l_i\}$ 
6: for  $P_i$  ( $1 \leq i \leq n$ ) in the descending order of  $l_i$  do
7:    $(\mathbf{v}, \mathbf{o}) \leftarrow \text{COMPACT}(L, \mathbf{v}, \mathbf{o}, P_i, 0)$ 
8:    $L \leftarrow \max_{1 \leq i \leq n} (x_i + \frac{l_i}{2})$ 
9: Return  $L, (\mathbf{v}, \mathbf{o})$ 
```

---

## 6 Computational results

The guided coordinate descent heuristics (GCDH) proposed in this paper were implemented with the C programming language and run on a single thread under a Mac PC with a 2.7 GHz Intel Xeon E5 processor and 64 GB memory. The performance of the GCDH was tested on two sets of instances for the ISP represented in the vector model. We converted these instances into the raster model with five different resolutions; i.e., we set the width  $W$  of the container  $C$  to 128,

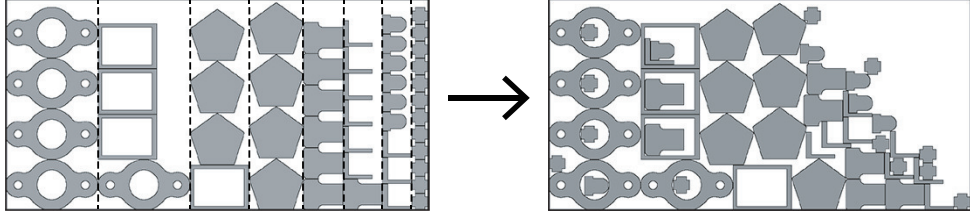


Figure 11: Constructing an initial solution for the ISP.

Table 1: The benchmark instances of the ISP

instance	#shapes	#pieces	avg.#lines	avg.#arcs	avg.#holes	degrees
Albano	8	24	6.83	0.00	0.00	0, 180 absolute
Dagli	10	30	7.30	0.00	0.00	0, 180 absolute
Dighe1	16	16	3.88	0.00	0.00	0 absolute
Dighe2	10	10	4.70	0.00	0.00	0 absolute
Fu	12	12	3.58	0.00	0.00	90 incremental
Jakobs1	25	25	6.00	0.00	0.00	90 incremental
Jakobs2	25	25	5.36	0.00	0.00	90 incremental
Mao	9	20	8.70	0.00	0.00	90 incremental
Marques	8	24	7.08	0.00	0.00	90 incremental
Shapes0	4	43	6.29	0.00	0.00	0 absolute
Shapes1	4	43	6.29	0.00	0.00	0, 180 absolute
Shirts	8	99	6.05	0.00	0.00	0, 180 absolute
Swim	10	48	20.0	0.00	0.00	0, 180 absolute
Trousers	17	64	5.94	0.00	0.00	0, 180 absolute
Profiles1	8	32	4.63	0.63	0.00	90 incremental
Profiles2	7	50	7.54	1.50	0.38	90 incremental
Profiles3	6	46	7.93	0.65	0.00	45 incremental
Profiles4	7	54	3.83	0.41	0.00	90 incremental
Profiles5	5	50	7.19	0.00	0.13	15 incremental
Profiles6	9	69	4.60	1.40	0.00	90 incremental
Profiles7	9	9	4.67	0.00	0.00	90 incremental
Profiles8	9	18	4.67	0.00	0.00	90 incremental
Profiles9	16	57	26.61	0.00	0.16	90 incremental
Profiles10	13	91	8.23	0.00	0.00	0 absolute

256, 512, 1024 and 2048 pixels. The first set includes 15 instances of the standard vector model without circular arcs nor holes (i.e., the simple polygon packing problem), which are available online at the web site of the working group on cutting and packing [ESICUP, 2003]. The second set includes 10 instances of an extended vector model, in which several instances incorporate circular arcs and holes into polygons [Burke et al., 2010]. Table 1 summarizes the data of the instances. The second column “#shapes” shows the number of different shapes, the third column “#pieces” shows the total number of pieces, the fourth column “avg.#lines” shows the average number of the line segments in an irregular shape, the fifth column “avg.#arcs” shows the average number of the circular arcs in an irregular shape, the sixth column “avg.#holes” shows the average number of holes in an irregular shape, and the seventh column “degrees” shows the permitted orientations, where we note that the permitted orientations are common to all pieces in the test instances.

Table 2 shows the computational results obtained by the GCDH, which are evaluated in the best and average density (%). We set the input parameters  $r_{\text{dec}} = 0.02$ ,  $r_{\text{inc}} = 0.005$  for the GCDH (Algorithm 1) and  $k_{\text{max}} = 200$  for the GLS (Algorithm 4). We tested the GCDH 10

Table 2: The density (%) of the proposed algorithm GCDH on the benchmark instances

instance	$W = 128\text{px}$		$W = 256\text{px}$		$W = 512\text{px}$		$W = 1024\text{px}$		$W = 2048\text{px}$	
	best	avg.	best	avg.	best	avg.	best	avg.	best	avg.
Albano	89.01	88.61	88.04	87.69	87.61	87.30	87.22	86.80	87.04	86.70
Dagli	87.96	87.09	86.84	86.07	86.32	85.49	86.27	85.42	85.92	85.14
Dighe1	91.36	88.48	96.07	95.55	97.60	97.47	98.81	98.69	99.33	99.20
Dighe2	93.01	93.01	95.01	94.77	97.28	97.17	98.79	98.74	99.28	99.20
Fu	91.45	90.61	90.56	89.93	90.33	89.33	90.39	89.64	89.30	88.82
Jakobs1	88.58	84.49	84.32	84.32	88.01	86.02	87.56	85.65	87.98	86.29
Jakobs2	81.33	80.67	81.91	78.77	79.51	78.52	79.24	78.12	79.31	78.23
Mao	87.17	86.43	85.12	84.60	84.84	83.48	84.03	83.38	83.63	82.88
Marques	91.39	91.39	89.92	89.51	90.43	89.19	89.36	88.69	88.52	88.14
Shapes0	68.49	67.38	66.74	66.17	65.55	65.02	65.10	64.25	64.81	64.25
Shapes1	75.30	74.04	73.38	72.50	72.35	71.71	71.88	71.08	71.46	71.00
Shirts	86.72	86.34	85.82	84.86	84.33	84.04	84.43	83.56	84.24	83.33
Swim	78.87	77.17	74.74	73.84	73.02	72.49	72.21	71.81	72.66	71.68
Trousers	88.97	88.13	87.98	87.08	87.42	86.59	88.02	86.59	87.40	86.76
Profiles1	84.74	84.65	86.03	84.69	86.93	84.46	84.32	83.37	85.73	84.04
Profiles2	79.43	79.06	77.42	76.90	77.28	76.18	76.27	75.91	75.98	75.33
Profiles3	76.32	74.72	74.27	73.52	73.87	72.82	73.51	72.22	72.65	71.77
Profiles4	86.04	84.90	85.92	85.02	85.13	84.41	85.31	84.38	84.64	83.89
Profiles5	83.88	82.98	81.53	81.23	81.66	81.07	82.10	80.72	81.47	80.96
Profiles6	81.40	80.66	81.14	80.11	79.03	78.54	77.50	76.78	77.94	76.54
Profiles7	87.25	87.25	92.59	92.40	95.80	95.65	98.27	98.18	98.92	98.83
Profiles8	87.34	85.08	84.47	84.02	85.73	84.62	86.65	84.90	88.50	85.38
Profiles9	66.95	66.07	61.08	60.10	57.59	57.05	56.64	55.53	55.53	54.59
Profiles10	70.90	70.27	68.75	68.31	68.20	67.33	67.91	66.85	67.14	66.43
avg.(1st)	85.69	84.56	84.75	83.98	84.61	83.84	84.52	83.74	84.35	83.69
avg.(2nd)	80.42	79.56	79.32	78.63	79.12	78.21	78.85	77.88	78.65	77.78
avg.(all)	83.49	82.48	82.48	81.75	82.33	81.50	82.16	81.30	82.06	81.22

times for each instance with the time limit of 1200 seconds for each run, which does not include the computation time of the preprocessing for generating NFPs for all pairs of different shapes and detecting corners for all generated NFPs (See Appendix in detail).

We first evaluated the effect of the corner detection technique on the GCDH. The fully implemented GCDH (with the corner detection) was 13.04 times faster on average than the naively implemented GCDH (without the corner detection) for the instances of high-resolution ( $W = 2048\text{px}$ ). It also brought the improvement in the quality of the obtained solutions; e.g., the fully implemented GCDH obtained 2.15 point better than the naively implemented GCDH in the average density (%) for the instances of high-resolution ( $W = 2048\text{px}$ ). The detailed computational results are shown in Appendix.

We next compared the computational results of the GCDH ( $W = 512\text{px}$ ) with those reported by Umetani et al. [2009] (denoted as “FITS”), Sato et al. [2019] (denoted as “ROMA”), and Burke et al. [2010] (denoted as “BLF”). The FITS and ROMA are a variant of the GCDH for the polygon packing problem, where the ROMA constrained the search space to place the pieces on a grid as same as Mundim et al. [2017], and computed the penetration depth efficiently via a variant of discretized Voronoi diagrams called the raster penetration map. Burke et al. [2010] considered an extended vector model incorporating circular arcs into polygons and proposed a robust orbital sliding method to compute NFPs. They developed a BLF algorithm that restricted the search space on vertical lines with sufficiently small gaps between them and incorporated it with local search and tabu search (TS) algorithms to find a good order of given pieces. Table 3

Table 3: The density (%) of FITS, ROMA, BLF and the proposed algorithm GCDH ( $W = 512\text{px}$ ) on the benchmark instances († We have corrected the density (%) based on their lengths  $L$  due to numerical errors in the literature.)

instance	FITS (vector)		ROMA (vector)		BLF <sup>†</sup> (vector)	GCDH (raster)	
	best	avg.	best	avg.	best	best	avg.
Albano	88.41	88.09	85.72	82.66	86.0	87.61	87.30
Dagli	87.76	87.26	88.73	87.25	82.2	86.32	85.49
Dighe1	99.90	99.89	100.00	100.00	82.1	97.60	97.47
Dighe2	100.00	100.00	100.00	100.00	84.3	97.28	97.17
Fu	92.14	91.56	91.94	91.94	89.2	90.33	89.33
Jakobs1	89.10	89.04	89.09	89.09	82.6	88.01	86.02
Jakobs2	80.56	80.43	87.73	82.53	75.1	79.51	78.52
Mao	85.19	84.43	83.61	81.08	78.7	84.84	83.48
Marques	90.65	89.88	91.02	89.87	86.5	90.43	89.19
Shapes0	67.35	66.76	68.79	68.72	65.5	65.55	65.02
Shapes1	73.76	73.07	76.73	75.86	71.5	72.35	71.71
Shirts	88.08	87.17	88.52	87.29	82.8	84.33	84.04
Swim	75.29	74.87	73.23	70.37	67.2	73.02	72.49
Trousers	90.19	89.74	90.75	90.36	86.9	87.42	86.59
Profiles1	—	—	—	—	82.5	86.93	84.46
Profiles2	—	—	—	—	73.8	77.28	76.18
Profiles3	—	—	—	—	70.8	73.87	72.82
Profiles4	—	—	—	—	86.8	85.13	84.41
Profiles5	—	—	—	—	75.9	81.66	81.07
Profiles6	—	—	—	—	72.1	79.03	78.54
Profiles7	—	—	—	—	73.3	95.80	95.65
Profiles8	—	—	—	—	78.7	85.73	84.62
Profiles9	—	—	—	—	52.9	57.59	57.05
Profiles10	—	—	—	—	65.0	68.02	67.33
avg.(1st)	86.31	85.87	86.84	85.50	80.0	84.61	83.84
avg.(2nd)	—	—	—	—	73.2	79.12	78.21
avg.(all)	—	—	—	—	77.2	82.33	81.50

shows their computational results, which are evaluated in the best and average density (%). We note that it is not appropriate to directly compare the density of these algorithms, because the GCDH was tested on the instances of the raster model while the other algorithms were tested those of the vector model. Table 4 shows the computational environment and the computation time (in seconds) of the algorithms. Burke et al. [2010] tested four variations of their algorithm, and each were run 10 times. Their results in Table 3 are the best results of 40 runs. They did not use time limit but stopped their algorithm by other criteria, and their computation time in Table 4 is the time spent to find the best solution reported in Table 3 in the run that found it; i.e., the time only one run is reported. Umetani et al. [2009] and Sato et al. [2019] tested their algorithms 10 times and 30 times for each instance, respectively, where they set the time limits for each run as shown in Table 4.

The GCDH obtained close results to other algorithms for the first set of instances despite it was tested on the raster model of high-resolution, where we note that the test instances of the vector model are represented by a small number of line segments. It also obtained that the better results than the BLF for the second set of instances. Figures 12 and 13 show the best layouts obtained by the GCDH for these instances ( $W = 512\text{px}$ ). These computational results illustrate that the GCDH attained a good performance for a wide variety of ISPs including

Table 4: The computation time of FITS, ROMA, BLF and the proposed algorithm GCDH on the benchmark instances (in seconds)

instance	FITS (vector)	ROMA (vector)	BLF (vector)	GCDH (raster)
	Xeon E5 2.7GHz	Core i9-7900X 3.3GHz	Pentium4 2.0GHz	Xeon E5 2.7GHz
	10 runs	30 runs	4 × 10 runs	10 runs
	limit	limit	to best	limit
Albano	1200	1200	299	1200
Dagli	1200	1200	252	1200
Dighe1	1200	600	3	1200
Dighe2	1200	600	148	1200
Fu	1200	600	139	1200
Jakobs1	1200	600	29	1200
Jakobs2	1200	600	51	1200
Mao	1200	1200	152	1200
Marques	1200	1200	21	1200
Shapes0	1200	1200	274	1200
Shapes1	1200	1200	239	1200
Shirts	1200	1200	194	1200
Swim	1200	1200	141	1200
Trousers	1200	1200	253	1200
Profiles1	—	—	15	1200
Profiles2	—	—	295	1200
Profiles3	—	—	283	1200
Profiles4	—	—	256	1200
Profiles5	—	—	300	1200
Profiles6	—	—	171	1200
Profiles7	—	—	211	1200
Profiles8	—	—	279	1200
Profiles9	—	—	98	1200
Profiles10	—	—	247	1200

circular arcs and holes.

## 7 Conclusion

We present an overlap minimization approach for the irregular strip packing problem (ISP) of the rasterized shapes that repeatedly solve the overlap minimization problem (OMP) as the core sub-problem while updating the length of the container. In this approach, we develop coordinate descent heuristics (CDH) for the OMP that repeats a line search in the horizontal and vertical directions alternately, where we propose a line search algorithm incorporating a pair of scanlines representation for the NFPs of the irregular shapes and a corner detection technique to improve its computational efficiency. The CDH are incorporated into a variant of the guided local search (GLS), which we call the guided coordinate descent heuristics (GCDH). Computational results show that the GCDH attained a good performance for the instances despite it was tested on the raster model of high-resolution. The proposed method in this paper enables us to develop practical software for a wide variety of free-form shape packing problems described in any format through the raster model.

## Acknowledgement

The authors would like to thank Yusuke Nakano for technical assistance with implementing the proposed algorithm GCDH especially for processing the raster model. This research did not receive any specific grant from funding agencies in the public, commercial, or not-for-profit sectors.

## References

- A. Albano and G. Sapuppo. Optimal allocation of two-dimensional irregular shapes using heuristic search methods. *IEEE Transactions on Systems, Man and Cybernetics*, 10:242–248, 1980. doi: 10.1109/TSMC.1980.4308483.
- R. Alvarez-Valdes, M. A. Caravilla, and J. F. Oliveira. Cutting and packing. In R. Martí, P. M. Pardalos, and M. G. C. Resende, editors, *Handbook of Heuristics*, chapter 31, pages 931–977. Springer, 2018. doi: 10.1007/978-3-319-07124-4\\_43.
- R. C. Art. *An approach to the two dimensional irregular cutting stock problem*. PhD thesis, Massachusetts Institute of Technology, 1966.
- A. R. Babu and N. R. Babu. A generic approach for nesting of 2-D parts in 2-D sheets using genetic and heuristic algorithms. *Computer-Aided Design*, 33:879–891, 2001. doi: 10.1016/S0010-4485(00)00112-3.
- J. A. Bennell and K. A. Dowsland. Hybridising tabu search with optimisation techniques for irregular stock cutting. *Management Science*, 47:1160–1172, 2001. doi: 10.1287/mnsc.47.8.1160.10230.
- J. A. Bennell and J. F. Oliveira. The geometry of nesting problems: A tutorial. *European Journal of Operational Research*, 184:397–415, 2008. doi: 10.1016/j.ejor.2006.11.038.
- J. A. Bennell and J. F. Oliveira. A tutorial in irregular shape packing problems. *Journal of the Operational Research Society*, 60:S93–S105, 2009. doi: 10.1057/jors.2008.169.
- J. A. Bennell and X. Song. A beam search implementation for the irregular shape packing problem. *Journal of Heuristics*, 16:167–188, 2010. doi: 10.1007/s10732-008-9095-x.
- J. Blazewicz, P. Hawryluk, and R. Walkowiak. Using a tabu search approach for solving the two-dimensional irregular cutting problem. *Annals of Operations Research*, 41:313–325, 1993. doi: 10.1007/BF02022998.
- E. K. Burke, R. S. R. Hellier, G. Kendall, and G. Whitwell. Irregular packing using the line and arc no-fit polygon. *Operations Research*, 58:948–970, 2010. doi: 10.1287/oper.1090.0770.
- P. Chen, Z. Fu, A. Lim, and B. Rodrigues. The two-dimensional packing problem for irregular objects. *International Journal on Artificial Intelligence Tools*, 13:429–448, 2004. doi: 10.1142/S0218213004001624.
- D. Dobkin, J. Hershberger, D. Kirkpatrick, and S. Suri. Computing the intersection-depth of polyhedra. *Algorithmica*, 9:518–533, 1993. doi: 10.1007/BF01190153.
- K. A. Dowsland, S. Vaid, and W. B. Dowsland. An algorithm for polygon placement using a bottom-left strategy. *European Journal of Operational Research*, 141:371–381, 2002. doi: 10.1016/S0377-2217(02)00131-5.

- H. Dyckhoff. A typology of cutting and packing problems. *European Journal of Operational Research*, 44:145–159, 1990. doi: 10.1016/0377-2217(90)90350-K.
- J. Egeblad, B. K. Nielsen, and A. Odgaard. Fast neighborhood search for two- and three-dimensional nesting problems. *European Journal of Operational Research*, 183:1249–1266, 2007. doi: 10.1016/j.ejor.2005.11.063.
- A. Elkeran. A new approach for sheet nesting problem using guided cuckoo search and pairwise clustering. *European Journal of Operational Research*, 231:757–769, 2013. doi: 10.1016/j.ejor.2013.06.020.
- ESICUP. The working group on cutting and packing within EURO. <https://www.euro-online.org/websites/esicup/>, 2003.
- A. M. Gomes and J. F. Oliveira. A 2-exchange heuristic for nesting problems. *European Journal of Operational Research*, 141:359–370, 2002. doi: 10.1016/S0377-2217(02)00130-3.
- A. M. Gomes and J. F. Oliveira. Solving irregular strip packing problems by hybridising simulated annealing and linear programming. *European Journal of Operational Research*, 171: 811–829, 2006. doi: 10.1016/j.ejor.2004.09.008.
- Y. Hu, S. Fukatsu, S. Imahori, and M. Yagiura. Efficient overlap detection and construction algorithm for the bitmap shape packing problem. *Journal of the Operations Research Society of Japan*, 61:132–150, 2018a. doi: 10.15807/jorsj.61.132.
- Y. Hu, H. Hashimoto, S. Imahori, and M. Yagiura. Practical algorithms for two-dimensional packing of general shapes. In T. F. Gonzalez, editor, *Handbook of Approximation Algorithms and Metaheuristics (second edition)*, chapter 33, pages 585–609. CRC Press, 2018b. doi: 10.1201/9781351236423.
- T. Imamichi, M. Yagiura, and H. Nagamochi. An iterated local search algorithm based on nonlinear programming for the irregular strip packing problem. *Discrete Optimization*, 6: 345–361, 2009. doi: 10.1016/j.disopt.2009.04.002.
- S. Jain and C. Gea. Two-dimensional packing problems using genetic algorithms. *Engineering with Computers*, 14:206–213, 1998. doi: 10.1115/96-DETC/DAC-1466.
- A. A. S. Leao, F. M. B. Toledo, J. F. Oliveira, M. A. Carraville, and R. Alvarez-Valdés. Irregular packing problems: A review of mathematical models. *European Journal of Operational Research*, 282:803–822, 2020. doi: 10.1016/j.ejor.2019.04.045.
- S. C. H. Leung, Y. Lin, and D. Zhang. Extended local search algorithm based on nonlinear programming for two-dimensional irregular strip packing problem. *Computers & Operations Research*, 39:678–686, 2012. doi: 10.1016/j.cor.2011.05.025.
- Z. Li and V. Milenkovic. Compaction and separation algorithms for non-convex polygons and their applications. *European Journal of Operational Research*, 84:539–561, 1995. doi: 10.1016/0377-2217(95)00021-H.
- L. R. Mundim, M. Andretta, and T. A. de Queiroz. A biased random key genetic algorithm for open dimensional nesting problems using no-fit raster. *Expert Systems with Applications*, 81: 358–371, 2017. doi: 10.1016/j.eswa.2017.03.059.
- H. Okano. A scanline-based algorithm for the 2D free-form bin packing problem. *Journal of the Operations Research Society of Japan*, 45:145–161, 2002. doi: 10.15807/jorsj.45.145.

- J. F. Oliveira and J. S. Ferreira. Algorithms for nesting problems. In R. V. V. Vaidel, editor, *Applied Simulated Annealing (Lecture Notes in Economics and Maths Systems)*, volume 396, pages 255–274. Springer, 1993. doi: 10.1007/978-3-642-46787-5\\_13.
- J. F. Oliveira, A. M. Gomes, and J. S. Ferreira. Topos — a new constructive algorithm for nesting problems. *OR Spectrum*, 22:263–284, 2000. doi: 10.1007/s002910050105.
- E. Rosten and T. Drummond. Machine learning for high-speed corner detection. In *European Conference on Computer Vision*, pages 430–443, 2006. doi: 10.1007/11744023\\_34.
- A. K. Sato, T. C. Martins, A. M. Gomes, and M. S. G. Tsuzuki. Raster penetration map applied to the irregular packing problem. *European Journal of Operational Research*, 279:657–671, 2019. doi: 10.1016/j.ejor.2019.06.008.
- G. Scheithauer. *Introduction to Cutting and Packing Optimization*. Springer, 2018. doi: 10.1007/978-3-319-64403-5.
- S. A. Segereich and L. M. P. F. Braga. Optimal nesting of general plane figures: A monte carlo heuristical approach. *Computers & Graphics*, 10:229–237, 1986. doi: 10.1016/0097-8493(86)90007-5.
- F. M. B. Toledo, M. A. Carraville, C. Ribeiro, and J. F. Oliveira. The dotted-board model: A new mip model for nesting irregular shapes. *International Journal of Production Economics*, 145:478–487, 2013. doi: 10.1016/j.ijpe.2013.04.009.
- S. Umetani, M. Yagiura, S. Imahori, T. Imamichi, K. Nonobe, and T. Ibaraki. Solving the irregular strip packing problem via guided local search for overlap minimization. *International Transactions in Operational Research*, 16:661–683, 2009. doi: 10.1111/j.1475-3995.2009.00707.x.
- C. Voudouris and E. Tsang. Guided local search and its application to the traveling salesman problem. *European Journal of Operational Research*, 113:469–499, 1999. doi: 10.1016/S0377-2217(98)00099-X.
- G. Wäscher, H. Haußner, and H. Schumann. An improved typology of cutting and packing problems. *European Journal of Operational Research*, 183:1109–1130, 2007. doi: 10.1016/j.ejor.2005.12.047.
- W. K. Wong, X. X. Wang, P. Y. Mok, S. Y. S. Leung, and C. K. Kwong. Solving the two-dimensional irregular objects allocation problems by using a two-stage packing approach. *Expert Systems with Applications*, 36:3489–3496, 2009. doi: 10.1016/j.eswa.2008.02.068.

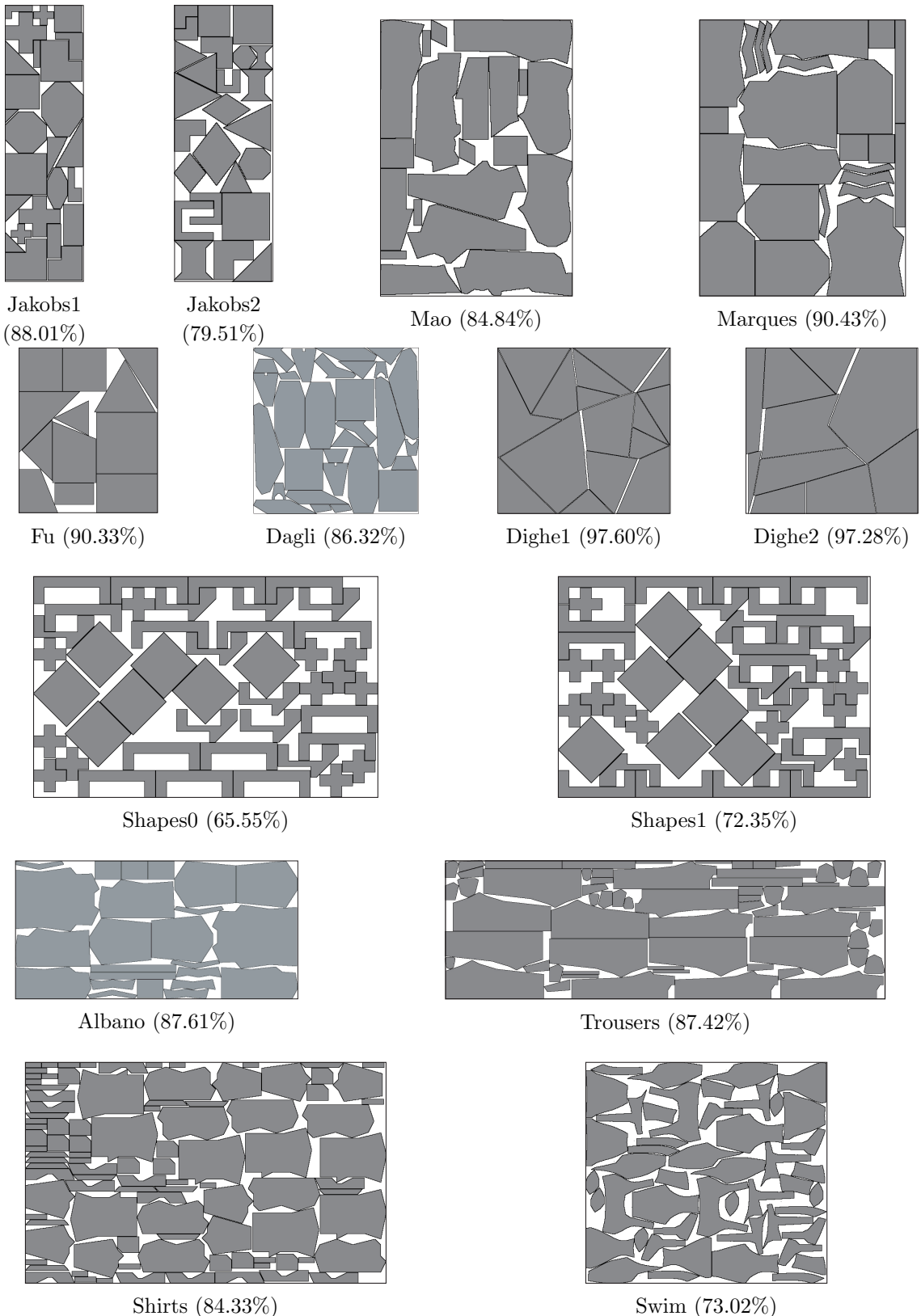


Figure 12: The best solutions for the test instances obtained by the proposed algorithm GCDH ( $W = 512\text{px}$ ).

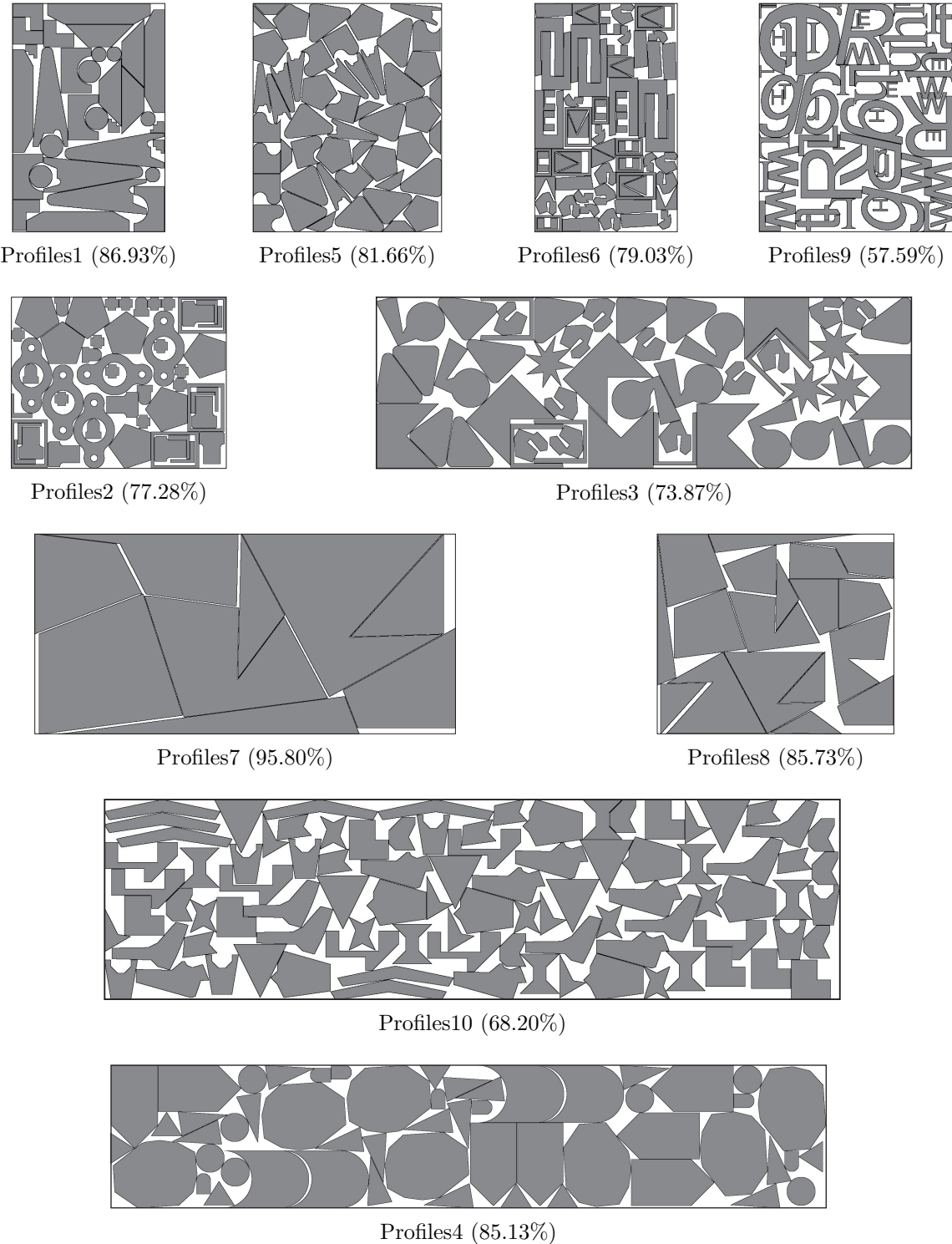


Figure 13: The best solutions for the test instances obtained by the proposed algorithm GCDH ( $W = 512\text{px}$ ).

## A Detailed computational results

This section contains the detailed computational results that are too long to make it into the paper. Tables 5 and 6 show the computation time of the preprocessing in seconds for generating NFPs for all pairs of different shapes and detecting corners for all generated NFPs. Tables 7 and 8 show to what extent the corner detection technique improves the performance of the GCDH. Table 7 shows the average factors in the computational efficiency so that that of the naively implemented GCDH (without the corner detection) is set to one.

Table 5: The computation time to generate NFPs (in seconds)

instance	$W = 128\text{px}$	$W = 256\text{px}$	$W = 512\text{px}$	$W = 1024\text{px}$	$W = 2048\text{px}$
Albano	0.05	0.19	0.79	3.22	13.09
Dagli	0.03	0.10	0.37	1.48	5.97
Dighe1	0.08	0.32	1.26	5.14	21.13
Dighe2	0.04	0.18	0.71	2.90	11.89
Fu	0.11	0.40	1.63	6.53	26.92
Jakobs1	0.08	0.26	0.95	3.59	14.56
Jakobs2	0.11	0.39	1.40	5.43	22.35
Mao	0.05	0.17	0.67	2.67	11.08
Marques	0.04	0.13	0.50	2.05	8.44
Shapes0	0.01	0.01	0.05	0.19	0.78
Shapes1	0.01	0.03	0.10	0.38	1.56
Shirts	0.01	0.04	0.15	0.57	2.32
Swim	0.03	0.10	0.40	1.58	6.43
Trousers	0.10	0.36	1.43	5.75	23.70
Profiles1	0.02	0.08	0.30	1.24	5.10
Profiles2	0.04	0.15	0.60	2.47	10.19
Profiles3	0.27	1.09	4.56	18.93	78.17
Profiles4	0.06	0.24	0.97	4.00	16.51
Profiles5	0.24	0.88	3.50	14.35	59.22
Profiles6	0.02	0.08	0.33	1.37	5.68
Profiles7	0.41	1.67	6.90	28.44	114.79
Profiles8	0.10	0.41	1.67	6.90	28.44
Profiles9	0.15	0.63	2.62	10.94	45.57
Profiles10	0.03	0.11	0.43	1.77	7.30
avg.(all)	0.09	0.33	1.35	5.49	22.55

Table 6: The computation time for the corner detection (in seconds)

instance	$W = 128\text{px}$	$W = 256\text{px}$	$W = 512\text{px}$	$W = 1024\text{px}$	$W = 2048\text{px}$
Albano	0.07	0.28	1.09	4.49	21.26
Dagli	0.05	0.14	0.51	2.10	9.28
Dighe1	0.12	0.45	1.85	7.90	39.61
Dighe2	0.07	0.25	1.00	4.82	22.19
Fu	0.23	0.64	2.27	9.74	63.48
Jakobs1	0.32	0.72	1.94	7.36	29.78
Jakobs2	0.36	0.77	2.38	8.95	37.44
Mao	0.14	0.36	1.26	5.09	23.31
Marques	0.09	0.26	0.88	3.59	16.66
Shapes0	0.01	0.02	0.08	0.30	1.35
Shapes1	0.01	0.04	0.15	0.61	2.77
Shirts	0.03	0.06	0.22	0.89	3.57
Swim	0.06	0.15	0.62	2.48	10.59
Trousers	0.13	0.39	1.21	4.93	23.07
Profiles1	0.06	0.16	0.49	1.80	8.27
Profiles2	0.07	0.17	0.57	2.19	11.55
Profiles3	0.40	1.50	5.16	20.94	107.79
Profiles4	0.11	0.37	1.38	6.74	34.84
Profiles5	0.76	1.75	6.31	18.06	75.97
Profiles6	0.05	0.11	0.30	1.13	4.70
Profiles7	0.59	2.20	9.98	55.08	240.45
Profiles8	0.18	0.59	2.25	10.04	55.37
Profiles9	0.26	0.67	2.28	8.09	35.27
Profiles10	0.05	0.15	0.58	2.27	10.64
avg.(all)	0.18	0.51	1.87	7.90	37.06

Table 7: The speed up factor of the proposed algorithm GCDH via the corner detection

instance	$W = 128\text{px}$	$W = 256\text{px}$	$W = 512\text{px}$	$W = 1024\text{px}$	$W = 2048\text{px}$
Albano	2.27	3.65	6.42	11.15	20.25
Dagli	1.59	2.44	4.13	7.06	12.86
Dighe1	1.87	2.73	4.41	7.22	11.92
Dighe2	2.08	3.58	6.10	10.02	17.31
Fu	2.25	3.89	7.04	12.72	23.24
Jakobs1	1.32	2.13	3.51	6.24	11.47
Jakobs2	1.19	2.11	3.56	5.58	9.16
Mao	1.32	2.15	3.47	5.84	10.21
Marques	1.58	2.55	4.06	6.45	12.11
Shapes0	1.49	2.39	4.36	7.71	13.16
Shapes1	1.70	2.18	3.85	6.52	10.84
Shirts	1.33	2.05	3.37	5.97	10.12
Swim	1.22	1.65	2.58	4.32	7.05
Trousers	2.12	3.61	6.66	10.93	18.10
Profiles1	1.28	1.66	3.36	6.13	9.93
Profiles2	1.27	1.85	3.33	5.67	9.11
Profiles3	1.49	2.26	3.66	6.87	9.66
Profiles4	2.77	4.28	7.61	12.78	24.18
Profiles5	1.13	1.57	2.46	4.57	7.78
Profiles6	1.14	1.63	2.31	3.61	5.73
Profiles7	3.25	5.36	9.50	15.46	28.50
Profiles8	1.82	3.05	4.88	9.02	14.28
Profiles9	1.03	1.43	2.06	2.98	5.05
Profiles10	1.59	2.61	4.56	7.26	10.92
avg.(all)	1.67	2.63	4.47	7.59	13.04

Table 8: The improvement in the density of the proposed algorithm GCDH via the corner detection

instance	$W = 128\text{px}$	$W = 256\text{px}$	$W = 512\text{px}$	$W = 1024\text{px}$	$W = 2048\text{px}$
Albano	0.13	-0.02	0.63	0.82	1.22
Dagli	0.06	0.10	0.56	1.38	1.56
Dighe1	1.36	5.56	7.14	12.50	14.64
Dighe2	0.00	-0.07	0.02	0.00	-0.01
Fu	0.58	0.50	1.14	1.47	1.74
Jakobs1	0.45	-0.47	2.44	3.12	3.35
Jakobs2	1.66	0.35	0.00	1.26	2.27
Mao	0.37	0.37	0.25	0.73	1.06
Marques	0.09	0.04	0.44	0.86	0.67
Shapes0	0.03	0.46	0.25	0.99	1.58
Shapes1	0.51	0.72	0.85	1.14	1.85
Shirts	-0.17	0.00	0.37	0.63	0.44
Swim	0.47	0.41	0.25	0.71	1.44
Trousers	0.38	0.36	0.73	1.15	1.29
Profiles1	-0.09	0.94	0.80	1.02	2.03
Profiles2	0.09	0.35	0.79	1.22	2.12
Profiles3	0.18	0.23	1.47	1.52	2.37
Profiles4	-0.05	1.08	1.14	1.74	2.18
Profiles5	-0.14	-0.36	0.57	0.74	1.93
Profiles6	0.00	-0.30	0.49	1.10	0.79
Profiles7	-0.03	-0.10	0.03	0.42	0.56
Profiles8	0.79	0.21	1.89	2.26	3.51
Profiles9	0.29	0.22	0.41	0.65	1.25
Profiles10	0.47	0.20	0.80	1.15	1.79
avg.(all)	0.31	0.45	0.98	1.61	2.15